Online Muscle Fatigue Estimation by Spectrum Tracking of the Maximal Contractions with sEMG

Kaan Gokcesu, Mert Ergeneci, Erhan Ertan, Hakan Gokcesu, Ahmad Zafar Khan

***Abstract*—The estimation of muscle fatigue and its analysis have seen a wide increase in its popularity because of its applicability to various applications. The most widely accepted and popular approach to monitor the local muscle fatigue is through the sEMG technology. The non-invasive nature, by itself, of this technology has been especially appealing to many fields, the most prominent ones of which are ergonomics and biomechanics. There are several approaches in literature to detect muscular exhaustion with the sEMG data. The most widely used techniques include the frequency-domain approaches and time-domain approaches. However, these techniques have certain limitations and may provide poor performance, especially under adversarial, corrupt data or even low SNR scenarios where the additive white Gaussian noise (AWGN) power is high. To this end, we propose a novel algorithm to track the muscle fatigue from the sEMG signal. Our approach consists of three successive stages, which are the detection of the maximal contractions, the tracking of their spectra, estimation of the fatigue. Through several experiments, we have validated our algorithms and illustrated better performance against the conventional methods.**

I. Introduction

Muscle fatigue, i.e., local muscle fatigue or neuromuscular fatigue, has various causes and can manifest itself in different forms or shapes. It occurs when the muscle lacks in oxygen, nutrition and undergoes a metabolic and structural change, and when the nervous system of the human anatomy loses its efficiency [1]–[3]. The detection and the tracking of the muscle fatigue has gained significant attention especially in the sports science and rehabilitation applications. These applications include the prevention of injury, the strength analysis, endurance development and performance monitoring [4]–[12].

The most straightforward way of monitoring muscle fatigue is to monitor the time when a subject is unable to perform a certain predetermined physically exhaustive task [13]–[16]. However, such a method is able to detect only the existence and not the extend of the muscle fatigue after a predetermined event. It provides no insight into the underlying process. Moreover, it is useless in the detection of the fatigue of a specific muscle when the task at hand requires the use of multiple muscles at the same time (since the observation will only be an aggregate result of all the muscles). Another method is to use lactate tests to measure the muscle fatigue, where blood samples can be taken with a specific interval during the time the task is performed. However, because of this procedure, it is not possible to track muscle fatigue in real time and generally with these tests one can detect the global not local fatigue of an individual.

On the other hand, the monitoring of the muscle fatigue in real time during a physical activity is possible by measuring the muscle activation potentials through the use of surface electromyography (sEMG) signals. The physiological changes that the muscles go through during fatigue are also reflected on the sEMG signals [17]. Hence, the sEMG signal is a paramount tool in the analysis of the muscle fatigue. Although, there are certain limitations in the application of the sEMG method to muscles below the skin and there can be some crosstalk of the sEMG signals from neighboring muscles, it is a widely used tool in detection of the local muscle fatigue due to its following advantages:

- non-invasiveness,
- local applicability,
- real-time monitoring,
- monitoring a particular muscle and
- correlation with physiological changes in fatiguing.

There are several methods to track the muscle fatigue that make use of the sEMG technology. These methods are frequency-domain approaches and time-domain approaches. When the muscle is fatigued, a shift is encountered in the frequency spectrum of the sEMG signal, which made the frequency-domain (spectral) approaches widely popular. The power spectral density (PSD) of the sEMG signal (i.e., power distribution of the sEMG signal across its frequency spectrum) has a nonrandom component. The PSD of the sEMG signal is dominant in the frequency band of 30-150 Hz. After 200 Hz, the power of the sEMG signal diminishes and just the AWGN remains. When the muscles start to get exhausted, the lactate and other ions such as H^+, Ca^{+2}, Na^+, and P^{-3} start to accumulate, which lessens the conductivity in the motor units of the muscle [18]–[20]. Thus, the number of impulses passing through the motor units during a specific interval decreases. Hence, when the muscle is fatigued, the PSD tends to shift to the lower frequencies.

Because of this important behavior in the PSD of the sEMG signal, methods such as mean frequency and median frequency analysis has gained increasing popularity since they can straightforwardly track the shift in the spectra (caused by local fatigue). Furthermore, one of the time-domain approaches, the zero crossing rate, is able to model the spectral shift as well, which is the reason it has also seen a wide

M. Ergeneci and E. Ertan is with Neurocess R&D Labs, Shenzhen, Guangdong, China, (e-mail: ergenecimert@gmail.com, erhertan@gmail.com).

K. Gokcesu is with the Department of Electrical Engineering and Computer Science, Cambridge, MA 02139, USA, (e-mail:gokcesu@mit.edu).

H. Gokcesu is with the Department of Electrical and Electronics Engineering, 06800, Bilkent, Ankara, Turkey, (e-mail:hgokcesu@ee.bilkent.edu.tr).

A. Z. Khan is with the Department of Electrical and Electronics Engineering, 06800, Bilkent, Ankara, Turkey, (e-mail:zafar.khan@ug.bilkent.edu.tr).

use. These three methods are the most prominent of the state-of-the-art [21]–[26]. However, these methods can be greatly affected by the amount of contractions, the AWGN power and motion artifacts. Hence, fatigue tracking with them may give misleading results under adversarial/noisy settings [27]–[29].

In this paper, we detail this problem of satisfactorily tracking the muscle fatigue over time. To this end, in order to overcome this obstacle, we propose a novel three-staged algorithm. Our algorithm first detects the maximal contractions in the sEMG signal, which contains the most reliable information about the muscle fatigue. After that, we track the spectra of the maximal contractions and decrease the effect of the AWGN. Lastly, we estimate and track the fatigue from these spectra. As we will show in the experiments, our algorithm can more accurately track the fatigue from the sEMG signal in comparison to the state-of-the-art.

The organization of the paper is organized as follows. In Section II, we first provide some necessary preliminaries about our problem. In Section III, we explain the contraction detection algorithm. In Section IV, the spectrum tracking approach is given with its benefits. In Section V, we detail our fatigue metric and how it is tracked. Next, in Section VI, the experiments are demonstrated, where we first validate algorithm by comparing it with the peak torque levels of the subjects. Then, we compare our algorithm with the state-of-the-art techniques to show that our algorithm can more accurately track the muscle fatigue. Finally, some concluding remarks are given in Section VII.

II. Preliminaries

In this paper, we are dealing with the problem of tracking the muscle fatigue. The tracking of the fatigue is done through the muscle activation potentials, which are extracted from the output of an sEMG sensor. In this section, we are providing some preliminaries that are required for our problem. In the first subsection, we first formally define the sEMG signal model. Then, in the second subsection, we are providing some details about the Spectrogram approach and the Short Time Fourier Transform (STFT). Finally, in the last subsection, we provide some details about the metric for fatigue tracking.

A. sEMG Signal

We formally define our problem by first modeling the sEMG signal. An observed sEMG signal can be mathematically modeled as the following:

$$x(t) = y(t) + v(t), \tag{1}$$

where $y(t)$ is the Muscle Activation Potential (MAP) and $v(t)$ is the Additive White Gaussian Noise (AWGN). Our aim is to track the fatigue of the muscle using the received signal $x(t)$.

We estimate the fatigue level of a muscle using its muscle activation potential $y(t)$. However, there is no guarantee that the muscle signals will be present at each observation (there may be times when the muscle is not in contraction). Hence, if there is no contraction at time t, then the observation will simply be given by $x(t) = v(t)$. Hence, we can summarize the model to a more concise form as

$$y(t) = c_t s(t) + v(t), \tag{2}$$

where $s(t)$ is the muscle contraction signal, $y(t) = c_t s(t)$ and c_t is 1 if there is a contraction and 0 otherwise.

Thus, we need to first find the observations that contain a contraction (i.e., we first need to estimate c_t). For this reason, our algorithm starts with a contraction detection method, which will be explained in detail in Section III. Our contraction detection algorithm uses the spectral behavior of the sEMG signal (i.e., changes in the frequency spectrum of the sEMG signal) to detect the contraction samples. To that end, we need to inspect the spectral behavior of the signal, which is done through the method of Spectrogram or STFT. Thus, in the next subsection, we explain this method in more detail.

B. Short Time Fourier Transform

To inspect the spectral behavior of the sEMG signals, we need to implement a frequency domain analysis. To extract the spectral components of the signal at hand, we use the conventional technique of Discrete Fourier Transform (DFT). The DFT of a signal $x(n)$ of length N (i.e., we have $x(n)$ for $n \in \{0, 1, \ldots, N-1\}$) is given by

$$X(k) = \sum_{n=0}^{N-1} x(n) \exp\left(-j\frac{2\pi kn}{N}\right). \tag{3}$$

To extract the temporal changes in the DFT, we utilize the Short Term Fourier Transform (STFT), which is a technique that includes taking the Fourier Transform of the signal with a sliding window. To avoid losing any temporal behavior, we use a sliding window with an overlap of $N-1$, i.e., the window slides only one sample in each successive transforms.

Let $X(t,k)$ be the k^{th} component of the Fourier transform of the signal whose window ends in the t^{th} sample. Thus,

$$X(t,k) = \sum_{n=0}^{N-1} x(n-N+1+t) \exp\left(-j\frac{2\pi kn}{N}\right). \tag{4}$$

The calculation of this transform with each incoming sample is very cumbersome. Therefore, next, we show how this can be calculated sequentially.

Remark 1. *The components of the STFT transform are sequentially calculable as*

$$X(t,k) = \left(X(t-1,k) - x(t-N) + x(t)\right) e^{j\frac{2\pi k}{N}}, \tag{5}$$

where N is the window length.

Proof. From (4), we have

$$X(t,k) \tag{6}$$

$$= \sum_{n=0}^{N-2} x(n-N+1+t) e^{-j\frac{2\pi kn}{N}} + x(t) e^{-j\frac{2\pi k(N-1)}{N}}, \tag{7}$$

$$= \left(X(t-1,k) - x(t-N) + x(t)\right) e^{j\frac{2\pi k}{N}}, \tag{8}$$

which concludes the proof. □

Hence, with STFT, we can sequentially quantify the temporal changes in the spectrum of the sEMG signal in an online manner. These spectra will be directly used in the contraction detection and the fatigue tracking as well. After some processing on these spectra, we will acquire a metric to quantify the muscle fatigue. In the next subsection, we explain what kind of conditions this metric needs to satisfy.

C. Muscle Fatigue

The muscle activation potential has a direct relationship to the current muscle fatigue $f(t)$. Our goal is to produce an estimate $\hat{f}(t)$ from the observed spectra $X(t,\cdot)$.

Quantification of the muscle fatigue is not a trivial problem. Therefore, the main interest is generally on the change in fatigue over time. Therefore, we need a metric that can satisfactorily model this change. The proportions between the changes in the muscle fatigue needs to be preserved as much as possible, so that we can determine how much the muscle is fatigued over time from our metric. Hence, any affine model of $\hat{f}(t)$ will provide us with the same information.

III. Contraction Detection

To correctly detect the EMG data frames with muscle contraction, we need to use some means of unsupervised learning procedure, since, in most prominent EMG applications, the muscle contraction times are not necessarily provided.

To decide whether an incoming data is part of a contraction or not we will compare some metric against a threshold τ_t. Let such metric at time t for sample $x(t)$ be m_t. Thus,

$$c_t = \begin{cases} 1, & m_t \geq \tau_t \text{ (active)} \\ 0, & m_t < \tau_t \text{ (inactive)} \end{cases}. \tag{9}$$

Hence, we will use the widely used thresholding technique (i.e., a linear separation on a one dimensional plane) for our detection/classification purposes [30]–[32].

A. Metric Design

The first part of the contraction detection algorithm includes the selection of the metric to be used for this classification, i.e., m_t. We will extract this metric from the STFT values $X(t,k)$. For that, we first take the Power Spectra of $X(t,\cdot)$. Since the EMG signal $x(t)$ is real, its DFT for an arbitrary window is conjugate symmetric. Hence, we only need the frequency components up to K, where K corresponds to the Nyquist frequency ($K = \lfloor N/2 \rfloor$). Hence, we take the power spectra as

$$P(t,k) = \|X(t,k)\|^2, \tag{10}$$

for $k \in \{0, 1, \ldots, K\}$.

The most straightforward metric is the total power in this spectra, which is given by

$$TP(t) = \sum_{k=0}^{K} P(t,k). \tag{11}$$

However, certain interference on the signal, especially the power line interference (PLI), can arbitrarily change the power spectra and adversely affect the total power. Moreover, certain interference caused by motion or impact artifacts can also have the same adverse effect. Therefore, using the total power may give erroneous understanding about the amount of EMG signal we are observing in the data. Fortunately, these kinds of interferences generally have a sinusoidal behavior (especially PLI). Henceforth, it is most suitable to choose a metric which is robust against the excessive/arbitrary increase in tight bands.

Thus, we use the mean log power of the spectra as

$$MLP(t) = \frac{1}{K+1} \sum_{k=0}^{K} \log(P(t,k)). \tag{12}$$

As can be seen, this metric is highly robust against certain frequency spikes and is prone to provide higher values for greater power across greater frequency bands. Since the logarithm reduces the multiplicative effects to additive, any arbitrary additive component will have minimal effect on this metric. This metric equals to the logarithm of the geometric mean of the power spectra as can be seen from (12). One aspect of this metric is its instability against very low components on the power spectra. Thus, a suitable smoothing parameter is useful such that MLP is given by

$$MLP(t) = \frac{1}{K+1} \sum_{k=0}^{K} \log(P(t,k) + \epsilon). \tag{13}$$

We set $\epsilon = 1$ to get nonzero metrics, which gives

$$MLP(t) = \frac{1}{K+1} \sum_{k=0}^{K} \log(P(t,k) + 1). \tag{14}$$

Hence, for our metric m_t in (9), we use $MLP(t)$, i.e.,

$$m_t = MLP(t). \tag{15}$$

B. Threshold Selection

After our metric design, we need an appropriate threshold, which we will use to compare our metric against and decide on the contraction samples. However, without the metric's distribution among the samples belonging to a contraction or noise, the selection of a static threshold in not trivial. To this end, we adopt a dynamic threshold selection, where we decide on an appropriate threshold in an adaptive manner.

To this end, we utilize a follow-the-leader based approach, where we decide on a best suitable threshold given all of the past data. However, the definition of a good threshold is not straightforward. Since the learning needs to be unsupervised, we need a clear definition for what makes a threshold good.

Note that, the fatigue information is most present during the maximal contractions. Given that our aim is to detect samples belonging to the maximal contraction phases, we need a sufficiently large threshold, which can cover most maximal contractions and disregard the rest. Since we are interested in a high enough threshold, the most straightforward way is to get the maximum observed metric up to present and add an appropriate decrease to that. So that

$$\tau_t = \max\{m_1, m_2, \ldots, m_t\} - \theta, \tag{16}$$

where θ is an appropriately chosen offset. However, the selection of this offset is nontrivial. Moreover, such an approach is prone to error in the existence of anomalies, adversarial or even noisy data.

To this end, instead of the $\max$ operation and a threshold θ, we adopt the following approach, which gives a threshold that is sufficiently high. The threshold is calculated as follows:

$$\tau_t = \frac{1}{K}\log\left(\frac{1}{t}\sum_{t'=1}^{t}\exp(Km_{t'})\right), \tag{17}$$

for some parameter $K \geq 0$. When this parameter approaches zero, τ_t approaches the mean of m_t up to time t, i.e., $\tau_t \to \frac{1}{t}\sum_{t'=1}^{t} m_{t'}$ when $K \to 0$. On the other hand, when this parameter approaches infinity, τ_t approaches the max of m_t up to time t, i.e., $\tau_t \to \max\{m_1, m_2, \ldots, m_t\}$ when $K \to \infty$. We use $K = 1$ for a sufficient balance between these extreme. This threshold calculation is similar in spirit to soft-max approach. While calculating this threshold from scratch is cumbersome, it is actually sequentially calculable as we show next.

Remark 2. *The threshold τ_t can be calculated sequentially as*

$$\tau_t = \log\left(\left(1-\frac{1}{t}\right)\exp(\tau_{t-1}) + \frac{1}{t}\exp(m_t)\right), \tag{18}$$

where m_t is the metric at time t.

Proof. From (17), we have

$$\tau_t = \log\left(\frac{1}{t}\sum_{t'=1}^{t-1}\exp(m_{t'}) + \frac{1}{t}\exp(m_t)\right), \tag{19}$$

$$= \log\left(\frac{t-1}{t}\exp(\tau_{t-1}) + \frac{1}{t}\exp(m_t)\right), \tag{20}$$

$$= \log\left(\left(1-\frac{1}{t}\right)\exp(\tau_{t-1}) + \frac{1}{t}\exp(m_t)\right), \tag{21}$$

which concludes our proof. □

IV. Spectrum Tracking

After detecting the frames with maximal contractions (i.e., $c_t = 1$), we use a Q-learning type approach to track their spectral behavior. Instead of directly using the observed $X(t,k)$ to represent the spectral behavior of the contractions, we start from an all zero $Y(t,k)$ and update it according to a learning rate λ_t as

$$Y(t,k) = (1-\lambda_t)Y(t-1,k) + \lambda_t X(t,k), \tag{22}$$

for $k \in \{0,1,\ldots,K\}$.

This approach can also be thought as modeling a dynamic ARMA process, where the autoregressive component comes from $Y(t-1,k)$ and the moving average component comes from $X(t,k)$ (which is the instantaneous spectrum at time t). Similarly, this model is equivalent to using Online Gradient Descent (OGD) under Mean Square Error (MSE) estimation, where λ_t corresponds to the learning rate [33], [34]. Moreover, it is also similar in spirit to exponential smoothing approach as well, where λ_t constitutes the smoothing parameter at time t.

Note that the spectral modeling in (22) is only done for the maximal contraction, i.e., when $c_t = 1$. Hence, the recursive update model in $Y(t,k)$ is actually given by

$$Y(t,k) = \begin{cases} (1-\lambda_t)Y(t-1,k) + \lambda_t X(t,k) & ,\text{if } c_t = 1 \\ Y(t-1,k) & ,\text{if } c_t = 0 \end{cases}, \tag{23}$$

or in a more compact form, we can represent (23) as

$$Y(t,k) = Y(t-1,k) + c_t\lambda_t(X(t,k) - Y(t,k)), \tag{24}$$

for $k \in \{0,1,\ldots,K\}$.

For efficient and adaptive tracking of the spectra, we utilize the log-window and set the learning rate as $\lambda_t = 1/\log_2(t+1)$. Note that, the log-window is stable enough to provide a near constant value and thus is suitable for adaptive update. Furthermore, one aspect of this modeling is its capability to decrease the noise in the system. Since the maximal contraction spectra can also contain some noise in them (especially AWGN noise), our approach is able to decrease it as we show in the next remark.

Remark 3. *Let $w(t)$ and $v(t) = (1-\alpha)w(t-1) + \alpha w(t)$. Let $w(t)$ be independent of each other and have the common variance σ^2. Then, the variance of $v(t)$ is upper-bounded as*

$$var(v(t)) \leq \alpha\sigma^2, \tag{25}$$

where $0 \leq \alpha \leq 1$.

Proof. Note that $v(t)$ can be written as

$$v(t) = \sum_{t'=1}^{t}\alpha(1-\alpha)^{t-t'}w(t'). \tag{26}$$

Since $w(t)$ are independent, the variance of $v(t)$ is given by

$$var(v(t)) = \sum_{t'=1}^{t} var(\alpha(1-\alpha)^{t-t'}w(t')), \tag{27}$$

$$= \sum_{t'=1}^{t}\alpha^2(1-\alpha)^{2t-2t'}\sigma^2, \tag{28}$$

$$= \alpha^2\frac{1-(1-\alpha)^{2t}}{1-(1-\alpha)^2}\sigma^2, \tag{29}$$

$$\leq \alpha\sigma^2, \tag{30}$$

since $0 \leq \alpha \leq 1$. □

From Remark 3, we can see that the noise in the spectra $X(t,n)$ will decrease from its initial value by a factor of the learning rate. Since the learning rate $\lambda_t = 1/\log_2(t+1)$ asymptotically converges to zero, the noise will diminish completely in infinity.

V. Fatigue Tracking

To detect the fatigue using the spectral behavior $Y(t,\cdot)$, we use the soft-max based approach and use the following metric

$$f(t) = \frac{\sum_{k=0}^{K}\exp\left(\theta\left\|Y(t,k)\right\|^2\right)k}{\sum_{k'=0}^{K}\exp\left(\theta\left\|Y(t,k')\right\|^2\right)}, \tag{31}$$

where the parameter θ is greater than 0. This metric gives much more weight to the frequency bins with more power, thus, approximates the peak value (or mode) of the spectra.

Remark 4. *One important aspect of this soft-max operation is that it is indifferent to any arbitrary offsets on the power spectra (which can be caused by the AWGN noise power.) Let us increase the AWGN noise power in the spectra by an amount of γ^2. Then, in expectation, the power spectra would be*

$$\left\|\widetilde{Y}(k,t)\right\|^2 = \|Y(k,t)\|^2 + \gamma^2. \tag{32}$$

Then, the equation in (31) *becomes*

$$\widetilde{f}(t) = \frac{\sum_{k=0}^{K} \exp\left(\theta \left\|\widetilde{Y}(t,k)\right\|^2\right) k}{\sum_{k'=0}^{K} \exp\left(\theta \left\|\widetilde{Y}(t,k')\right\|^2\right)}, \tag{33}$$

$$= \frac{\sum_{k=0}^{K} \exp\left(\theta(\|Y(t,k)\|^2 + \gamma^2)\right) k}{\sum_{k'=0}^{K} \exp\left(\theta(\|Y(t,k')\|^2 + \gamma^2)\right)}, \tag{34}$$

$$= \frac{\sum_{k=0}^{K} \exp\left(\theta \|Y(t,k)\|^2\right) k}{\sum_{k'=0}^{K} \exp\left(\theta \|Y(t,k')\|^2\right)}, \tag{35}$$

$$= f(t). \tag{36}$$

Thus, our metric is robust against the noise power.

To avoid the problem of excessive weighting in the presence of arbitrary, adversarial frequency components, we need to carefully select the parameter θ. Let θ be such that

$$\theta \|Y(t,k)\|^2 << 1 \tag{37}$$

Thus, the weights are

$$1 \leq \exp(\theta \|Y(t,k)\|^2) << e, \tag{38}$$

and excessive weighting does not occur.

Additionally, we put $f(t)$ through a first order exponential smoothing, similar to in Section IV as

$$s_t = (1-\lambda)s_{t-1} + \lambda f_t, \tag{39}$$

where $0 \leq \lambda \leq 1$ is the smoothing parameter.

Remark 5. *Let us take a sliding window of length L. Then, with the first order exponential smoothing, the coefficient of $f(t)$ in $s(t)$ will be λ (i.e., the newest sample in our window). The coefficient of $f(t-L+1)$ will be $\lambda(1-\lambda)^{L-1}$. The parameter λ that maximizes this coefficient is*

$$\arg\max_{\lambda} \lambda(1-\lambda)^{L-1} = \frac{1}{L}, \tag{40}$$

and the coefficient of $f(t-L+1)$ is

$$\lambda(1-\lambda)^{L-1} \geq \frac{1}{eL}. \tag{41}$$

Since the coefficient of $f(t)$ is $\lambda = 1/L$, the smoothing also approximates the uniform weighting (or averaging) over a window of length L (or $1/\lambda$).

Proof.

$$\max \lambda(1-\lambda)^{L-1} = \max\left(\log(\lambda) + (L-1)\log(1-\lambda)\right) \tag{42}$$

We take the derivative and set it to zero since the objective function is convex. Hence, let

$$\arg\max_{\lambda} \lambda(1-\lambda)^{L-1} = \lambda^*. \tag{43}$$

Then, since the derivative of $\log(x)$ is $1/x$, we have

$$\frac{1}{\lambda^*} = \frac{L-1}{1-\lambda^*}, \tag{44}$$

$$\lambda^* = \frac{1}{L}. \tag{45}$$

Hence, the weight of the newest sample is $1/L$, and the weight of the oldest sample in the L-length window is given by

$$\lambda^*(1-\lambda^*)^{L-1} = \frac{1}{L}\left(1-\frac{1}{L}\right)^{L-1}, \tag{46}$$

$$\geq \frac{e^{-1}}{L}\left(1-\frac{1}{L}\right)^{-1}, \tag{47}$$

$$\geq \frac{1}{eL}, \tag{48}$$

which concludes the proof. □

Remark 6. *This approach will put more emphasis on the fatigue metrics of contractions with larger power. The Taylor Series expansion of $\exp(\theta \|Y(t,k)\|^2)$ according to $\theta \|Y(t,k)\|^2$ around 0 is*

$$\exp(\theta \|Y(t,k)\|^2) = 1 + \theta \|Y(t,k)\|^2 + \frac{1}{2}\theta^2 \|Y(t,k)\|^4 + \dots \tag{49}$$

From (49)*, we have*

$$\exp(\theta \|Y(t,k)\|^2) \geq 1 + \theta \|Y(t,k)\|^2. \tag{50}$$

From (37) *and $\sum_{n=2}^{\infty} \frac{1}{n!} = e - 2$, we also have*

$$\exp(\theta \|Y(t,k)\|^2) << 1 + (e-1)\theta \|Y(t,k)\|^2. \tag{51}$$

Hence, we can say that

$$\exp(\theta \|Y(t,k)\|^2) \approx 1 + \theta \|Y(t,k)\|^2. \tag{52}$$

Therefore,

$$f(t) \approx \frac{\sum_{k=0}^{K}(1 + \theta \|Y(t,k)\|^2)k}{\sum_{k'=0}^{K}(1 + \theta \|Y(t,k')\|^2)}, \tag{53}$$

$$\approx \frac{\sum_{k=0}^{K}(1 + \theta \|Y(t,k)\|^2)k}{K+1}, \tag{54}$$

since $\theta \|Y(t,k)\|^2 << 1$. Thus, from (54)*, we have*

$$f(t) \approx \frac{K}{2} + \frac{\theta}{K+1}\sum_{k=0}^{K} \|Y(t,k)\|^2 k, \tag{55}$$

$$\approx \frac{K}{2} + \frac{\theta P^*(t)}{K+1} m^*(t), \tag{56}$$

where $P^*(t)$ is the total power and $m^*(t)$ is the mean frequency of the spectrum at time t. From (39)*, we have*

$$s(t) \approx \frac{K}{2} + \sum_{t'=0}^{t} \frac{\theta\lambda(1-\lambda)^{t-t'}}{K+1} P^*(t) m^*(t). \tag{57}$$

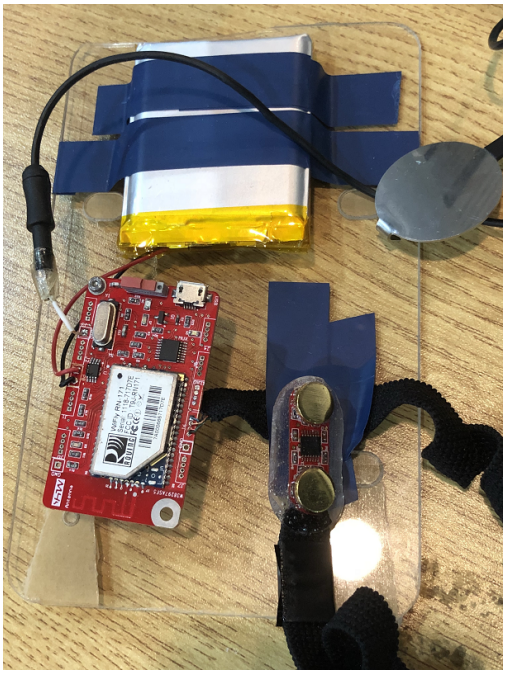

Figure 1: The active sEMG sensor.

Subject No	Age	Gender	Height (cm)	Weight (kg)
1	24	Male	167	72
2	24	Male	173	72
3	20	Female	167	61
4	25	Male	189	66
5	25	Male	178	68
6	24	Female	169	67
7	26	Female	165	58
8	24	Male	175	78
9	28	Male	168	70
10	24	Female	181	60

Table I: Gender, age, height, weight information of the subjects

Thus, if we only look at the relevant temporally dynamic (changing) affine model of the series $s(t)$, we have

$$\sum_{t'=0}^{t}(1-\lambda)^{t-t'}P^*(t)m^*(t), \tag{58}$$

which gives exponentially decreasing weights to the values further in the past. Hence, we approximately track $P^*(t)m^*(t)$ and our metric will be more biased towards the mean frequency of the contractions closer to the maximal contraction.

VI. Experiments

In this section, we collect sEMG sensor data from ten subjects and process the acquired sEMG signals to track the muscle fatigue levels. In the first subsection, we detail the experiment setup. First, the hardware used in our experiments is explained. Then, the physical activity done by the subjects are detailed. After the collection of the sEMG data, in the second subsection, we first validate the performance of our algorithm, where we compare the output of our algorithm against the peak torque level collected during the experiments. Once we have validated our algorithm, we move on to compare it against the state-of-the-art fatigue tracking algorithms in the third subsection, where we compare the outputs of our algorithm against the methods: the Mean Frequency, the Median Frequency and the Zero Crossing Rate.

A. Experiment Setup

In our experiments, we collect sEMG data from our subjects with an active sEMG sensor, which is shown in Figure 1. The collected sEMG data is required to analyze, estimate and track our subjects local muscle fatigue levels.

1) sEMG Sensor: Our sEMG sensor design is based on the dry-active sEMG sensor architecture.

- We use disc shaped electrodes to acquire the muscle signal from their skin contact. These electrodes have copper core and they are gold plated to increase the conductivity and durability.
- We manufacture the electrodes in accordance with the SENIAM standards [35], where they have a diameter of 10 mm and an inner electrode distance of 20 mm.
- The electrodes are connected to an industry level instrumentation amplifier to acquire their voltage difference.
- After that, the output of the instrumentation amplifier is passed through a quasi high-pass filter and a gain amplifier to have a total gain of 500.
- After that, we put the signal through a band-pass filter with a passband of $20-450$ Hz.
- We cover our sEMG sensor with epoxy to seal them. This provides water resistance and further robustness.

2) Data Acquisition Unit: To collect data from this sensor we need an additional data acquisition unit.

- We send the output of the sEMG sensor to the data acquisition unit through textile based litz wire cables, which provide increased flexibility and high stretchability.
- In the data acquisition unit the signal is sampled using an ADC with 12-bit resolution every 1 milliseconds.
- The collected samples are sent with WiFi to MATLAB.

3) Data Collection: Using our sensor, we collect sEMG data from 10 healthy subjects with varying physiques (i.e. age, gender, height (cm) and weight (kg)), which are summarized in Table I. During the experiments, subjects realized isometric contractions of 7 sets, where each set required them to complete 10 push and 10 pull exercises using an isokinetic dynamometer.

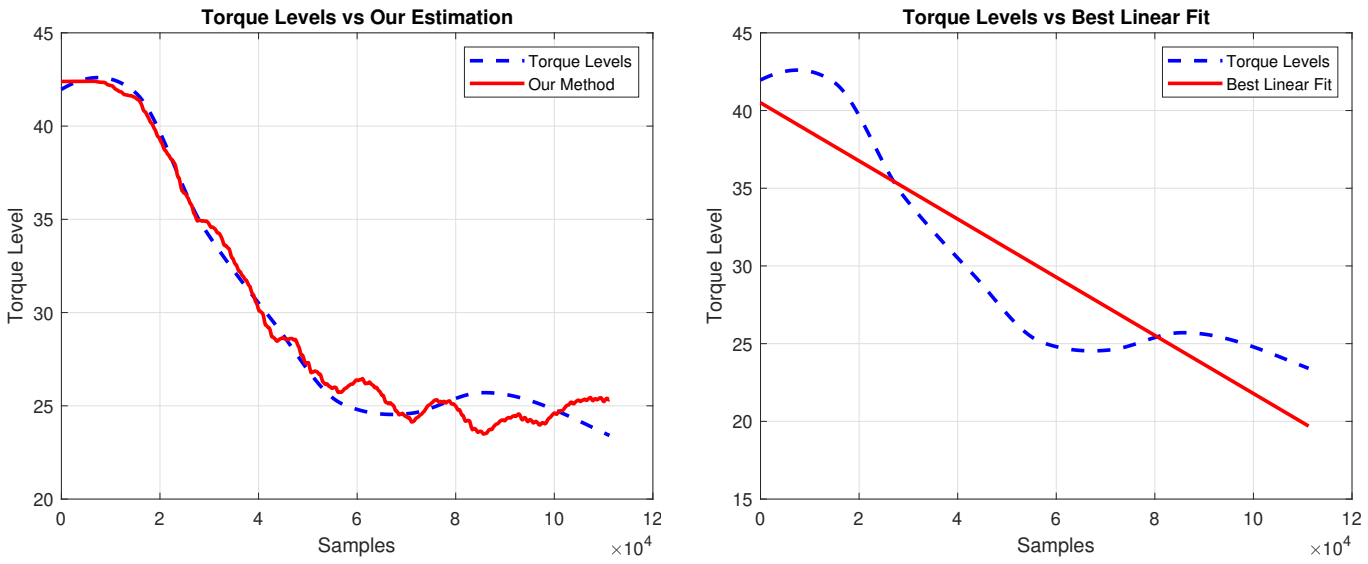

(a) (b)

Figure 2: (a) Comparison of the torque levels and the least squares fit of our algorithm for Subject 1. (b) Comparison of the torque levels and the best linear least squares fit for Subject 1.

B. Validation

To validate our algorithms, we collect peak torque levels from our subjects during their exercises. We then interpolate the collected torque levels to the whole experiment duration.

Quantification of the muscle fatigue is non-trivial. Therefore, we are mainly interested in the relative changes of muscle fatigue over time. Hence, we need a metric that can model these changes and preserve relative proportions between these changes as much as possible. With this metric, we can determine how much the muscle is fatigued over time. To that end, we are using a least-squares fitting based approach to compare our estimations with the actual indicator of fatigue levels, which is the peak torque levels in the maximal contractions.

1) The Least Squares Fitting: Let $g(t)$ be an estimation of the fatigue at time t and let $h(t)$ be an actual indicator of the fatigue level at time t. To compare whether or not these estimations are a good indicator for the fatigue, we need to look at them from a common perspective. We assume that $h(t)$ is an affine function of the actual muscle fatigue $f(t)$. Thus,

$$h(t) = a_h f(t) + b_h. \tag{59}$$

Since we have no knowledge of the parameters a_h, b_h. We try to model $h(t)$ itself instead of $f(t)$. Hence, we choose parameters a^* and b^* such that

$$(a^*, b^*) = \arg\max_{(a,b)} \sum_{t=1}^{T} (h(t) - ag(t) - b)^2, \tag{60}$$

where T is the time horizon. Then, we have the estimation of the indicator $h(t)$, which is given by

$$\tilde{h}(t) = a^* g(t) + b^*. \tag{61}$$

2) Comparison Against the Best Linear Fit: In sEMG analysis, linear models are widely used to estimate fatigue levels. For example, after extracting the mean or median frequency from the collected data, a linear fitting is done to model the behavior of the cumulative change in fatigue. However, such approaches are not usable for sufficient modeling and tracking of changes in the fatigue levels during short time periods. Because of their low modeling power, linear models can be insufficient. To observe this, we have fitted a linear function to the torque levels. This linear function is the best linear fit with the best bias and rate. Since this linear fit has problems modeling the changes in the torque level, linear modeling done on any arbitrary metric to model the fatigue will have insufficient modeling capabilities. In Figure 2a, 2b, we can see that while our method is able to track the changes in the torque levels, a linear model is not able to track them satisfactorily.

C. Comparisons

We compare our algorithm against the conventional techniques the mean frequency, the median frequency and the zero crossing rate. All of the algorithms use the same contraction detection algorithm, because otherwise these algorithms have very poor performance.

1) Mean Frequency: The mean frequency, i.e., MN_t, at time t is calculated from the mean of the frequency according to the probability mass function (which constitutes a probability simplex) created from the power spectral density of the spectrum $X(t, \cdot)$. Let

$$P(t,k) = \frac{\|X(t,k)\|^2}{\sum_{k'=0}^{K} \|X(t,k')\|^2}, \tag{62}$$

where $P(t, \cdot)$ is the power spectral density. Hence, $\sum_{k=0}^{K} P(t,k) = 1$, and $P(t, \cdot)$ is a probability simplex. With $P(t, \cdot)$, we can calculate MN_t as

$$MN_t = \sum_{k=0}^{K} kP(t,k), \tag{63}$$

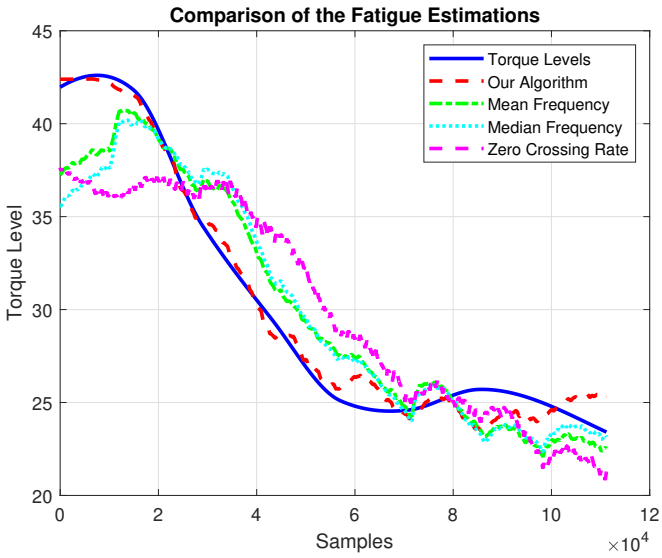

Figure 3: The Comparison of the Fatigue Estimations.

which gives the average of the random variable whose probability mass function corresponds to the PSD, $P(t,\cdot)$, of $X(t,\cdot)$. We use exponential smoothing on the mean frequency as

$$MN_t = (1-\lambda)MN_{t-1} + \lambda\sum_{k=0}^{K} kP(t,k). \tag{64}$$

2) Median Frequency: In order to estimate the median frequency at time t, MD_t, we calculate the cumulative sum $C(t,k)$ of $P(t,k)$ as

$$C(t,k) = \sum_{k'=0}^{k} P(t,k'), \tag{65}$$

for $k \in \{0,1,2,\ldots,K\}$. Let k^* be the index of the first component in $C(t,\cdot)$ that is greater than 0.5, i.e.,

$$C(t,k^*-1) \leq \frac{1}{2} < C(t,k^*). \tag{66}$$

Then, MD_t is given by

$$MD_t = k^* - 1 + \frac{0.5 - C(t,k^*-1)}{C(t,k^*) - C(t,k^*-1)}, \tag{67}$$

$$= k^* - \frac{C(t,k^*) - 0.5}{C(t,k^*) - C(t,k^*-1)} \tag{68}$$

To observe the smooth changes in the median frequency, we again use exponential smoothing as

$$MD_t = (1-\lambda)MD_{t-1} + \lambda\left(k^* - \frac{C(t,k^*) - 0.5}{C(t,k^*) - C(t,k^*-1)}\right) \tag{69}$$

3) Zero Crossing Rate: The zero crossing rate of $x(t)$ is calculated as the proportion of the number of times the signal crosses zero to the total number of times. Let

$$d(t) = \frac{1 - sign(x(t)x(t-1))}{2}, \tag{70}$$

where $sign(\cdot)$ is 1 if the argument is greater than or equal to zero and -1 otherwise. Hence, $d(t)$ in (70) gives whether or not a zero crossing event occurred. To observe the smooth changes in the zero crossing rate, we use exponential smoothing. Hence, the zero crossing rate, $ZC(t)$ is given by

$$ZC(t) = (1-\lambda)ZC(t-1) + \lambda d(t), \tag{71}$$

$$= (1-\lambda)ZC(t-1) + \lambda\frac{(1 - sign(x(t)x(t-1)))}{2}, \tag{72}$$

from (70).

For all of the algorithms and our method the smoothing parameter is set as $\lambda = 1/30000$ to approximately average half minute time windows. As can be seen in Figure 3, thanks to the exponential smoothing all of the algorithms can more or less track the changes in fatigue levels. However, the best affine fit extracted from the mean frequency, the median frequency and the zero crossing rate still show some deviations from the torque levels. Our model on the other hand has substantially better similarity with the torque levels. In Table II, we have listed the Mean Absolute Error (MAE), Root Mean Square Error (RMSE), Mean Absolute Percentage Error (MAPE) and Root Mean Square Percentage Error of all of the algorithms. As can be seen the MAE and MSE of our method are substantially better than the others. While the mean frequency is the best after our technique, the zero crossing rate has the lowest modeling capabilities. For the percentage errors, while our method has on average approximately 3% error, the mean frequency has $\approx 7\%$, the median frequency has $\approx 7.5\%$ and the zero crossing rate has $\approx 10.5\%$ error. Thus, our algorithm has better overall performance because of its superior modeling capabilities.

Methods	**Our Method**	**Mean Frequency**	**Median Frequency**	**Zero Crossing Rate**
Mean Absolute Error	0.66716	2.006	2.1902	3.0226
Root Mean Square Error	0.86621	2.2954	2.6722	3.5098
Mean Absolute Percentage Error	2.4948 %	6.6839 %	7.0506 %	9.8585 %
Root Mean Square Percentage Error	3.3901 %	7.4025 %	8.1247 %	11.123 %

Table II: Average Errors of the Fatigue Estimations for all subjects

VII. Conclusion

In this paper, we introduced a three-staged algorithm, where we first detected the maximal contractions in the sEMG signal. For muscle fatigue, these are the most informative and reliable parts of the signal. Then, we tracked the spectra of the maximal contractions, which decreased the effect of the AWGN. Finally, the fatigue was estimated and tracked from these spectra. Because of its superior modeling capabilities, our algorithm was able to more accurately track the fatigue from the sEMG signal in comparison to the best linear fit and the conventional techniques used with our contraction detection.

References

[1] R. Merletti, P. A. Parker, and P. J. Parker, *Electromyography: physiology, engineering, and non-invasive applications*. John Wiley & Sons, 2004, vol. 11.

[2] D. B. Chaffin, "Localized muscle fatigue—definition and measurement," *Journal of Occupational and Environmental Medicine*, vol. 15, no. 4, pp. 346–354, 1973.

[3] M. Cifrek, V. Medved, S. Tonković, and S. Ostojić, "Surface emg based muscle fatigue evaluation in biomechanics," *Clinical biomechanics*, vol. 24, no. 4, pp. 327–340, 2009.

[4] Y. Fan and Y. Yin, "Active and progressive exoskeleton rehabilitation using multisource information fusion from emg and force-position epp," *IEEE Transactions on Biomedical Engineering*, vol. 60, no. 12, pp. 3314–3321, Dec 2013.

[5] R. I. Pettigrew, W. J. Heetderks, C. A. Kelley, G. C. Y. Peng, S. H. Krosnick, L. B. Jakeman, K. D. Egan, and M. Marge, "Epidural spinal stimulation to improve bladder, bowel, and sexual function in individuals with spinal cord injuries: A framework for clinical research," *IEEE Transactions on Biomedical Engineering*, vol. 64, no. 2, pp. 253–262, Feb 2017.

[6] B. J. E. Misgeld, M. Lüken, R. Riener, and S. Leonhardt, "Observer-based human knee stiffness estimation," *IEEE Transactions on Biomedical Engineering*, vol. 64, no. 5, pp. 1033–1044, May 2017.

[7] X. Navarro-Sune, A. L. Hudson, F. D. V. Fallani, J. Martinerie, A. Witon, P. Pouget, M. Raux, T. Similowski, and M. Chavez, "Riemannian geometry applied to detection of respiratory states from eeg signals: The basis for a brain;ventilator interface," *IEEE Transactions on Biomedical Engineering*, vol. 64, no. 5, pp. 1138–1148, May 2017.

[8] K. M. Vamsikrishna, D. P. Dogra, and M. S. Desarkar, "Computer-vision-assisted palm rehabilitation with supervised learning," *IEEE Transactions on Biomedical Engineering*, vol. 63, no. 5, pp. 991–1001, May 2016.

[9] M. Sartori, D. G. Llyod, and D. Farina, "Neural data-driven musculoskeletal modeling for personalized neurorehabilitation technologies," *IEEE Transactions on Biomedical Engineering*, vol. 63, no. 5, pp. 879–893, May 2016.

[10] Y. Bai, D. Do, Q. Ding, J. A. Palacios, Y. Shahriari, M. M. Pelter, N. Boyle, R. Fidler, and X. Hu, "Is the sequence of superalarm triggers more predictive than sequence of the currently utilized patient monitor alarms?" *IEEE Transactions on Biomedical Engineering*, vol. 64, no. 5, pp. 1023–1032, May 2017.

[11] E. Gaeta, G. Cea, M. T. Arredondo, and J. P. Leuteritz, "Amirtem: A functional model for training of aerobic endurance for health improvement," *IEEE Transactions on Biomedical Engineering*, vol. 59, no. 11, pp. 3155–3161, Nov 2012.

[12] M. Ergeneci, K. Gokcesu, E. Ertan, and P. Kosmas, "An embedded, eight channel, noise canceling, wireless, wearable semg data acquisition system with adaptive muscle contraction detection," *IEEE Transactions on Biomedical Circuits and Systems*, vol. 12, no. 1, pp. 68–79, Feb 2018.

[13] H. Liu, "Exploring human hand capabilities into embedded multifingered object manipulation," *IEEE Transactions on Industrial Informatics*, vol. 7, no. 3, pp. 389–398, Aug 2011.

[14] R. Chattopadhyay, M. Jesunathadas, B. Poston, M. Santello, J. Ye, and S. Panchanathan, "A subject-independent method for automatically grading electromyographic features during a fatiguing contraction," *IEEE Transactions on Biomedical Engineering*, vol. 59, no. 6, pp. 1749–1757, June 2012.

[15] R. H. Edwards, "Human muscle function and fatigue," *Human muscle fatigue: physiological mechanisms*, pp. 1–18, 1981.

[16] N. K. Vøllestad, "Measurement of human muscle fatigue," *Journal of neuroscience methods*, vol. 74, no. 2, pp. 219–227, 1997.

[17] C. L. De, "Myoelectrical manifestations of localized muscular fatigue in humans." *Critical reviews in biomedical engineering*, vol. 11, no. 4, pp. 251–279, 1984.

[18] A. V. Boxtel and L. R. B. Schomaker, "Motor unit firing rate during static contraction indicated by the surface emg power spectrum," *IEEE Transactions on Biomedical Engineering*, vol. BME-30, no. 9, pp. 601–609, Sept 1983.

[19] M. M. Lowery and M. J. O'Malley, "Analysis and simulation of changes in emg amplitude during high-level fatiguing contractions," *IEEE Transactions on Biomedical Engineering*, vol. 50, no. 9, pp. 1052–1062, Sept 2003.

[20] R. Merletti and D. Farina, *Muscle Force and Myoelectric Manifestations of Muscle Fatigue in Voluntary and Electrically Elicited Contractions*. Wiley-IEEE Press, 2016, pp. 592–. [Online]. Available: http://ieeexplore.ieee.org/xpl/articleDetails.jsp?arnumber=7471089

[21] K. Gokcesu, M. Ergeneci, E. Ertan, A. Z. Alkilani, and P. Kosmas, "An semg-based method to adaptively reject the effect of contraction on spectral analysis for fatigue tracking," in *Proceedings of the 2018 ACM International Symposium on Wearable Computers, UbiComp 2018, Singapore, Singapore, October 8-12, 2018*, 2018, pp. 80–87. [Online]. Available: http://doi.acm.org/10.1145/3267242.3267292

[22] E. Koutsos and P. Georgiou, "An analogue instantaneous median frequency tracker for emg fatigue monitoring," in *2014 IEEE International Symposium on Circuits and Systems (ISCAS)*, June 2014, pp. 1388–1391.

[23] B. H. Zhou, P. Liu, N. B. Liu, X. H. Wu, R. Lu, and X. M. Ni, "Median frequency of surface emg signal of antagonist muscles during repeated contractions," in *1992 14th Annual International Conference of the IEEE Engineering in Medicine and Biology Society*, vol. 4, Oct 1992, pp. 1626–1627.

[24] A. J. Fuglevand, D. A. Winter, A. E. Patla, and D. Stashuk, "Effect of increased motor unit action potential duration on the amplitude and mean power frequency of the electromyogram," in *Images of the Twenty-First Century. Proceedings of the Annual International Engineering in Medicine and Biology Society,*, Nov 1989, pp. 953–954 vol.3.

[25] S. R. Alty and A. Georgakis, "Mean frequency estimation of surface emg signals using filterbank methods," in *2011 19th European Signal Processing Conference*, Aug 2011, pp. 1387–1390.

[26] R. Merletti, D. Biey, M. Biey, G. Prato, and A. Orusa, "On-line monitoring of the median frequency of the surface emg power spectrum," *IEEE Transactions on Biomedical Engineering*, vol. BME-32, no. 1, pp. 1–7, Jan 1985.

[27] K. Gokcesu, M. Ergeneci, E. Ertan, and H. Gokcesu, "An adaptive algorithm for online interference cancellation in emg sensors," *IEEE Sensors Journal*, pp. 1–1, 2018.

[28] O. Sayli and A. Akin, "Investigation of the usage of averaged instantaneous frequency parameter along with mean and median frequency in electromyogram (emg) analysis," in *Proceedings of the IEEE 13th Signal Processing and Communications Applications Conference, 2005.*, May 2005, pp. 597–600.

[29] R. B. R. Manero, A. Shafti, B. Michael, J. Grewal, J. L. R. Fernández, K. Althoefer, and M. J. Howard, "Wearable embroidered muscle activity sensing device for the human upper leg," in *2016 38th Annual International Conference of the IEEE Engineering in Medicine and Biology Society (EMBC)*, Aug 2016, pp. 6062–6065.

[30] I. Delibalta, K. Gokcesu, M. Simsek, L. Baruh, and S. S. Kozat, "Online anomaly detection with nested trees," *IEEE Signal Processing Letters*, vol. 23, no. 12, pp. 1867–1871, Dec 2016.

[31] D. Dere, M. Ergeneci, and K. Gokcesu, "An online adaptive classification of google trends data anomalies for investor sentiment analysis." pp. 79–81, 2018.

[32] K. Gokcesu and S. S. Kozat, "Online anomaly detection with minimax optimal density estimation in nonstationary environments," *IEEE Transactions on Signal Processing*, vol. 66, no. 5, pp. 1213–1227, March 2018.

[33] M. Zinkevich, "Online convex programming and generalized infinitesimal gradient ascent." in *ICML*, T. Fawcett and N. Mishra, Eds. AAAI Press, 2003, pp. 928–936.

[34] K. Gokcesu and S. S. Kozat, "Online density estimation of nonstationary sources using exponential family of distributions," *IEEE Transactions on Neural Networks and Learning Systems*, vol. 29, no. 9, pp. 4473–4478, Sept 2018.

[35] SENIAM, "Sensor placement," http://www.seniam.org/bicepsbrachii.html.